

AD-A058 141

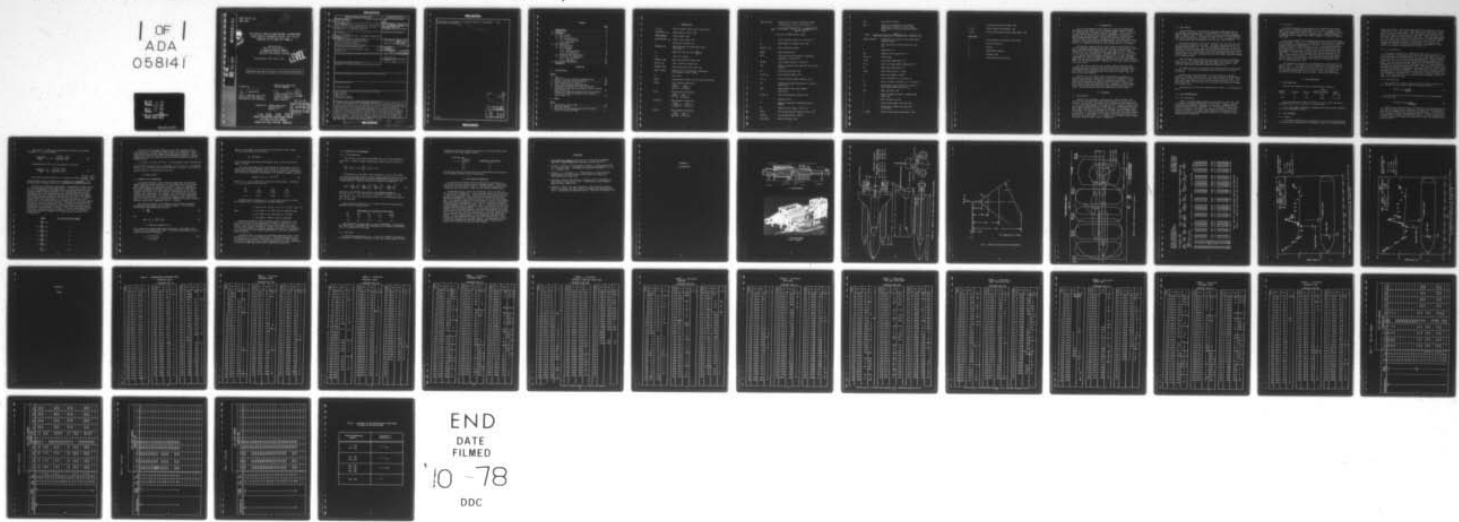
ARNOLD ENGINEERING DEVELOPMENT CENTER ARNOLD AIR FORCE--ETC F/G 22/2
TEST RESULTS FROM THE NASA/ROCKWELL INTERNATIONAL SPACE SHUTTLE--ETC(U)
JUN 78 K W NUTT

UNCLASSIFIED

AEDC-TSR-78-V15

NL

1 OF 1
ADA
058141



END
DATE
FILED
10-78
DDC

AU No.
DDC FILE COPY

ADA058141

AEDC-TSR-78-V15
JUNE 1978



TEST RESULTS FROM THE NASA/ROCKWELL INTERNATIONAL
SPACE SHUTTLE INTEGRATED VEHICLE TEST (IH 85)
CONDUCTED IN THE AEDC-VKF TUNNEL A

B029096
2 H
Kenneth W. Nutt
ARO, Inc., AEDC Division
A Sverdrup Corporation Company
von Kármán Gas Dynamics Facility
Arnold Air Force Station, Tennessee

Period Covered: April 19-26, 1978

LEVEL III

APPROVED FOR PUBLIC RELEASE; DISTRIBUTION UNLIMITED.

Reviewed by:

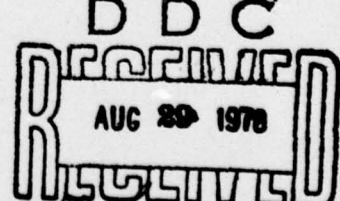
Ervin P. Jaskolski

ERVIN P. JASKOLSKI, Capt, USAF
Test Director, VKF Division
Directorate of Test Operations

Approved for Publication:
FOR THE COMMANDER

Chauncey D. Smith, Jr.
CHAUNCEY D. SMITH, JR, Lt Colonel, USAF
Director of Test Operations
Deputy for Operations

Prepared for: Johnson Space Center
(NASA-JSC)(ES3)
Houston, TX



78 08 28 1274A
ARNOLD ENGINEERING DEVELOPMENT CENTER
AIR FORCE SYSTEMS COMMAND
ARNOLD AIR FORCE STATION, TENNESSEE

UNCLASSIFIED

REPORT DOCUMENTATION PAGE		READ INSTRUCTIONS BEFORE COMPLETING FORM
1. REPORT NUMBER AEDC-TSR-78-V15	2. GOVT ACCESSION NO.	3. RECIPIENT'S CATALOG NUMBER 9
4. TITLE (and Subtitle) Test Results from the NASA/Rockwell International Space Shuttle Integrated Vehicle Test (IH 85) Conducted in the AEDC-VKF Tunnel A.		5. TYPE OF REPORT & PERIOD COVERED Final Report, April 1, 1978 April 26, 1978
7. AUTHOR(s) Kenneth W. Nutt, ARO, Inc., a Sverdrup Corporation Company		6. PERFORMING ORG. REPORT NUMBER
9. PERFORMING ORGANIZATION NAME AND ADDRESS Arnold Engineering Development Center Air Force Systems Command Arnold Air Force Station, TN 37389		10. PROGRAM ELEMENT, PROJECT, TASK AREA & WORK UNIT NUMBERS Program Element 921E-01 17 62-02F
11. CONTROLLING OFFICE NAME AND ADDRESS Johnson Space Center (NASA-JSC) (ES3) Houston, TX		12. REPORT DATE June 1978 11
14. MONITORING AGENCY NAME & ADDRESS (if different from Controlling Office)		13. NUMBER OF PAGES 44 12-44p
		15. SECURITY CLASS. (of this report) Unclassified
		15a. DECLASSIFICATION DOWNGRADING SCHEDULE N/A
16. DISTRIBUTION STATEMENT (of this Report) Approved for public release; distribution unlimited.		
17. DISTRIBUTION STATEMENT (of the abstract entered in Block 20, if different from Report)		
18. SUPPLEMENTARY NOTES Available in DDC		
19. KEY WORDS (Continue on reverse side if necessary and identify by block number) Heat Transfer Space Shuttle Supersonic Testing Interference Heating		
20. ABSTRACT (Continue on reverse side if necessary and identify by block number) Tests were conducted in the AEDC-VKF Supersonic Wind Tunnel A to obtain convective heat-transfer-rate distributions on the Space Shuttle Integrated Vehicle during simulated first and second stage conditions of the flight profile. The test model was a 0.0175-scale model (60-OTS), of the Rockwell International Vehicle 5 configuration. Model configurations tested included the Integrated Vehicle and the Orbiter/External Tank with the Solid Rocket Boosters removed. The tests were conducted at Mach numbers 3 and 4 using the thin-skin thermocouple technique. The model was tested at angles of attack of 0, ±2.5, and		

+ or -

UNCLASSIFIED

± 5 deg and at yaw angles of 0, ± 3 , ± 4.5 , ± 5 , ± 7.5 , and ± 9 deg. A test description is presented.

+ or -

+ or -

ACCESSION BY	
NAME	DATE SERVED
SFC	SFC CO-HR
DISTRIBUTION/AVAILABILITY	
DISTRIBUTOR/RELEASER	
DISTRIBUTION/AVAILABILITY	
DATE AVAIL FOR RELEASE	
APRIL 1987	APRIL 1987

+ or -

AFSC
Arnold AFB Tenn

UNCLASSIFIED

CONTENTS

	<u>Page</u>
NOMENCLATURE	2
1.0 INTRODUCTION	6
2.0 APPARATUS	
2.1 Test Facility	6
2.2 Test Article	7
2.3 Test Instrumentation	
2.3.1 Test Conditions	7
2.3.2 Test Data	8
3.0 TEST DESCRIPTION	
3.1 Test Conditions	8
3.2 Test Procedure	
3.2.1 General	8
3.2.2 Data Acquisition	9
3.2.3 Data Reduction	9
3.3 Adiabatic Wall Temperature	11
3.4 Uncertainty of Measurements	
3.4.1 Test Conditions	13
3.4.2 Test Data	14
4.0 DATA PACKAGE PRESENTATION	14
REFERENCES	15

APPENDIXES

A. ILLUSTRATIONS

Figure

1. Tunnel A	17
2. Sketch of the Space Shuttle Integrated Model	18
3. External Tank Nose Tip Configuration	19
4. Model Installation in Tunnel A	20
5. Typical Heat-Transfer Data Tabulation	21
6. Comparison of External Tank Data for the OTS Configuration with Theory and Results from a Previous Test at Mach 3.01	22
7. Comparison of External Tank Data for the OTS Configuration with Theory and Results from a Previous Test at Mach 4.02	23

B. TABLES

Table

1. Thermocouple Constant Sets	25
2. Test Data Summary	37
3. Equations for Calculating Local Surface Angle of Attack on the Orbiter Model	41

NOMENCLATURE

a_1, a_2, a_3	Denote constant terms used to calculate R
ALPHA-MODEL, α_m	Model angle of attack, deg
ALPHA-PREBEND	Sting prebend, deg
ALPHA-SECTOR, α_s	Tunnel sector angle, deg
b	Model wall thickness, ft
CONSTANT SET	Identification of thermocouple hookup (see Table 1)
c_p	Model wall specific heat, $\frac{\text{Btu}}{\text{lbm} \cdot ^\circ\text{R}}$
C.R.	Center of rotation
DELTABF, DABF	Body flap deflection angle, deg
DELTAE, DAE	Elevon deflection angle, deg
DELTASB, DASB	Speed brake deflection angle, deg
DTWDT, $d\text{TW}/dt$	Derivative of the model wall temperature with respect to time, $^\circ\text{R/sec}$
FS	Full scale
GROUP	Identification number for each tunnel injection
H(TAW)	Heat-transfer coefficient, $\frac{\text{QDOT}}{\text{TAW} - \text{TW}} \quad \frac{\text{Btu}}{\text{ft}^2 \cdot \text{sec} \cdot ^\circ\text{R}}$
H(TO)	Heat-transfer coefficient, $\frac{\text{QDOT}}{\text{TO} - \text{TW}} \quad \frac{\text{Btu}}{\text{ft}^2 \cdot \text{sec} \cdot ^\circ\text{R}}$
H(0.95TO)	Heat-transfer coefficient, $\frac{\text{QDOT}}{(0.95\text{TO}) - \text{TW}} \quad \frac{\text{Btu}}{\text{ft}^2 \cdot \text{sec} \cdot ^\circ\text{R}}$
H(RTO)	Heat-transfer coefficient, $\frac{\text{QDOT}}{(\text{RTO}) - \text{TW}} \quad \frac{\text{Btu}}{\text{ft}^2 \cdot \text{sec} \cdot ^\circ\text{R}}$

HREF, HREF-FR	Reference heat-transfer coefficient based on Fay-Riddell theory, Btu/ft ² -sec-°R
HREF =	$\frac{8.17173(P_01)^{0.5} (\mu_0)^{0.4} [1 - (P_{-INF}/P_01)]^{0.25}}{(RN)^{0.5} (T_0)^{0.15}}$
	$\times [0.2235 + 0.0000135 [T_0 + 560]]$
L	Axial reference length, in. (see Fig. 2)
M _e	Mach number at boundary layer edge
MACH NO., M _∞	Free stream Mach number
MODEL	Model configuration
MU-0	Viscosity conditions based on stagnation temperature, lbf-sec/ft ²
MU-INF	Free-stream viscosity, lb-sec/ft ²
OTS	Orbiter, external tank, and both solid rocket boosters
OT	Orbiter and external tank
P-INF, P _∞	Free-stream pressure, psia
P ₀ , P ₀	Tunnel stilling chamber pressure, psia
P ₀₁	Stagnation pressure downstream of a normal shock, psia
QDOT	Heat-transfer rate, wbc _p (DTWDT), Btu/ft ² -sec
Q-INF, q _∞	Free-stream dynamic pressure, psia
r	Recovery factor
R	Radius or analytical temperature ratio, TAW/T ₀
RN	Reference nose radius, (0.0175 ft)
RE/FT	Free-stream Reynolds number per foot, ft ⁻¹
RHO-INF	Free-stream density, lbm/ft ³
ROLL-MODEL	Model roll angle, deg

SRB	Solid Rocket Booster
STFR	Theoretical stagnation point Stanton number for a 0.0175-ft (1 scale foot) radius sphere calculated from Fay-Riddell theory
STFR =	$\frac{H_{REF}}{(RHO-INF)(V-INF)[0.2235 + 0.0000135(T_0 + 560)](32.174)}$
SWITCH POSITION	Designates the position of the thermocouple selector switch
t	Time from start of model injection cycle, sec
T	Temperature, °R
TAW	Adiabatic wall temperature, °R
TC-NO, T/C	Thermocouple
T-INF	Free-stream temperature, °R
T ₀ , T _o	Tunnel stilling chamber temperature, °R
TW	Model wall temperature, °R
V-INF	Free-stream velocity, ft/sec
w	Model wall density, lbm/ft ³
X	Axial coordinate, in. (see Fig. 2)
Y ₀	Orbiter lateral coordinate, in. (see Fig. 2)
X/L	Thermocouple axial location as a ratio of model length from model nose tip
YAW	Model yaw angle, deg
β	Angle of sideslip, equal to negative yaw angle, deg
γ	Ratio of specific heat
δ	Local surface angle of attack, deg
ε	Combination of model roll angle and θ or ψ, deg
θ, THETA	External tank angular measurement, deg

λ	Local model deflection angle, deg
ϕ , PHI	Orbiter angular measurement, deg
ψ , PSI	Solid rocket booster angular measurement, deg

Subscripts

e	Flow properties at boundary layer edge
i	Initial conditions
o	Orbiter
s	Solid Rocket Booster
t	External tank
∞	Free-stream flow properties

1.0 INTRODUCTION

The work reported herein was conducted at the Arnold Engineering Development Center (AEDC), Air Force Systems Command (AFSC), by ARO, Inc., AEDC Division (a Sverdrup Corporation Company), contract operator of AEDC, AFSC, Arnold Air Force Station, Tennessee. The work was sponsored by the Johnson Space Center (NASA-JSC(ES3)), Houston, Texas, under Program Element 921E-01. Rockwell International (RI), Space Division, Downey, California was responsible for test planning and data analysis. The project monitor for NASA-JSC(ES3) was Mrs. Dorothy B. Lee and the test engineer for Rockwell International was Mr. Jim Cummings.

The test was conducted in the 40-in. Supersonic Wind Tunnel (A) at the von Karman Gas Dynamics Facility (VKF) during the period April 19-26, 1978, under ARO Project Number V41A-W5. Data were recorded at Mach numbers 3 and 4 at free stream unit Reynolds numbers of 3.7×10^6 and 4.1×10^6 per foot, respectively. The model angle of attack varied from -5 to 5 deg with model yaw angles varying from -9 to 9 deg. Two model configurations; the OTS configuration composed of the fully integrated model with the orbiter, external tank (ET) and both solid rocket boosters (SRB), and the OT Configuration consisting of the orbiter and the external tank, were tested.

The objective of the test was to obtain updated supersonic heat-transfer rate distributions on the Space Shuttle Vehicle configuration VC72-000002F during simulated first and second stage conditions. Data were recorded from instrumentation on the orbiter, external tank and both solid rocket boosters.

Copies of all the detailed test logs have been transmitted to Rockwell International. Three copies of the final tabulated data are being transmitted with this report to Rockwell International. A data tape will be transmitted to Chrysler Corporation Space Division for their analysis under the Dataman contract. Inquiries to obtain copies of the test data should be directed to NASA-JSC(ES3), Houston, Texas 77058. A microfilm record has been retained in the VKF at AEDC.

2.0 APPARATUS

2.1 TEST FACILITY

Tunnel A is a continuous, closed-circuit, variable density wind tunnel with an automatically driven flexible-plate-type nozzle and a 40-by 40-in. test section. The tunnel can be operated at Mach numbers from 1.5 to 6 at maximum stagnation pressures from 29 to 200 psia, respectively, and stagnation temperatures up to 750°R ($M_\infty = 6$). Minimum operating pressures range from about one-tenth to one-twentieth of the maximum at each Mach number. The tunnel is equipped with a model injection system which allows removal of the model from the test section while the tunnel remains in operation. A description of the tunnel and airflow calibration information may be found in Ref. 1. A schematic view of Tunnel A and the model injection system is shown in Fig. 1, Appendix A.

2.2 TEST ARTICLE

The 60-OTS model is a 0.0175-scale thin-skin thermocouple model of the Rockwell International Vehicle 5 configuration. The model was supplied by Rockwell International. A sketch of the Space Shuttle Integrated model is shown in Fig. 2. The model was constructed of 17-4 PH stainless steel with a nominal skin thickness of 0.030 in. at the instrumented areas. All thermocouples were spot-welded to the thin skin inner surface.

Data were obtained for the orbiter, external tank, and both the right and left SRB (as viewed by the pilot). Two model configurations were investigated during this test. The fully integrated model with the orbiter, external tank, and both the right and left SRB was designated the OTS configuration. The OT configuration consisted of only the orbiter and external tank combination with the forward and aft SRB attachments installed on the external tank. The model configurations are listed under the model headings in the tabulated data.

The spike nose tip (10-deg sharp cone) was installed on the external tank, Fig. 3. The external tank reference length of 32.295 in. in model scale is based on the tank length with the nipple nose attached. This reference length was retained for consistent values of X/L.

The inboard elevons on the orbiter were deflected down 10-deg throughout the test. The orbiter speedbrakes and body flap were set at zero deflection.

Boundary layer trips were used on the orbiter and on each SRB to generate a turbulent boundary layer. The trips consisted of 0.020-in.-diam balls spaced on 0.060-in. centers around a form fitted steel strip. The trips were located at an X/L of 0.04 on the orbiter nose and 0.19 on the nose of each SRB. The nose shape on the external tank effectively tripped the boundary layer.

The installation of the OTS configuration in Tunnel A is illustrated in Fig. 4.

2.3 TEST INSTRUMENTATION

2.3.1 Test Conditions

Tunnel A stilling chamber pressure is measured with a 15-, 60-, 150-, or a 300-psid transducer referenced to a near vacuum. Based on periodic comparisons with secondary standards, the accuracy (a bandwidth which includes 95 percent of the residuals, i.e. 2σ deviation) of these transducers is estimated to be within ± 0.2 percent of reading or ± 0.015 psi, whichever is greater. Stilling chamber temperature is measured with a copper-constantan thermocouple with an accuracy of $\pm 3^\circ\text{F}$ based on repeat calibrations (2σ deviation).

2.3.2 Test Data

The model temperatures were measured with iron-constantan thermocouples with an estimated uncertainty of ± 0.5 percent. Data from over 1000 thermocouples were recorded during the test. A Beckman® 210 analog-to-digital converter was used in conjunction with a Digital Equipment Corp.® (DEC) PDP-11 Computer and a DEC-10 Computer to record the temperature data.

Data from a maximum of 97 thermocouples can be recorded during each tunnel injection. Twelve sets of thermocouples were required to accomodate the large number of thermocouples on this test. These sets are called Constant Sets in the tabulated data. A list of the twelve Constant Sets is given in Table I. This list includes all of the thermocouples that were installed for the test. Several of the listed thermocouples were determined to be inoperative and these have been omitted from the tabulated data. A total of three Constant Sets could be connected at one time. A three position selector switch was used to select the desired Constant Set for each injection. A new series of three Constant Sets could be readily connected using quick disconnect thermocouple plugs with 15 thermocouples per plug.

The dimensional locations of the thermocouples at each position are given in Table I. The angular reference system for the thermocouples is shown in Fig. 2. It is important to note that the top centerline of the external tank and both SRB's is the 0-deg location. This agrees with the reference system used in the IH-72 test. The bottom centerline was used as the 0-deg position on the IH-41, IH-41A, and IH-41B tests.

3.0 TEST DESCRIPTION

3.1 TEST CONDITIONS

The test was conducted at the following nominal conditions:

MACH NO.	P ₀ , psia	T ₀ , °R	H _{REF} , sec·ft ² ·°R	Btu RE/FT
3.01	37	720	0.055	3.8×10^6
4.02	70	720	0.050	4.1×10^6

Data were obtained at angles of attack of 0, ± 2.5 , and ± 5 deg and at yaw angles ($-\beta$) of 0, ± 3 , ± 4.5 , ± 5 , ± 7.5 , and ± 9 deg.

A test data summary showing all configurations tested and the variables for each is presented in Table 2.

3.2 TEST PROCEDURE

3.2.1 General

In the VKF continuous flow wind tunnels (A, B, C), the model is mounted on a sting support mechanism in an installation tank directly underneath the

tunnel test section. The tank is separated from the tunnel by a pair of fairing doors and a safety door. When closed, the fairing doors, except for a slot for the pitch sector, cover the opening to the tank and the safety door seals the tunnel from the tank area. After the model is prepared for a data run, the personnel access door to the installation tank is closed, the tank is vented to the tunnel flow, the safety and fairing doors are opened, and the model is injected into the airstream. After the data are recorded, the model is retracted into the tank and the sequence is reversed with the tank being vented to atmosphere to allow access to the model in preparation for the next run.

3.2.2 Data Acquisiton

The initial step prior to recording the test data was to cool the model uniformly to approximately 60°F with cooled high pressure air. This was accomplished by providing chilled air from a vortex generator (Hilsch vortex tube, Ref. 2) to a retractable cooling manifold. With the model attitude set at zero pitch the cooling manifold was positioned around the model. Once the cooling cycle was complete the cooling manifold was retracted and the model attitude was established prior to tunnel injection. The model was then injected into the tunnel. When the model reached tunnel centerline, the model was immediately translated forward to clear an area of tunnel induced shock impingement. The thermocouple outputs were scanned approximately 15 times per second starting prior to model injection into the airstream and continuing about 5 seconds after the model reached centerline. After each injection, the cooling cycle was repeated to cool the model to an isothermal state.

3.2.3 Data Reduction

The reduction of thin-skin thermocouple data normally involves only the calorimetric heat balance which in coefficient form is:

$$H(TAW) = wbc_p \frac{dT_W/dt}{TAW-TW} \quad (1)$$

For this test a value of 0.95 TO was selected for TAW and equation (1) can be written

$$H(0.95TO) = wbc_p \frac{dT_W/dt}{0.95TO-TW} \quad (2)$$

Radiation and conduction losses are neglected in this heat balance and data reduction simply requires evaluation of dT_W/dt from the temperature-time data and determination of model material properties. For the present tests, radiation effects were negligible; however, conduction effects can be significant in several regions of the models. To permit identification of these regions and to improve evaluation of the data, the following procedure was used.

Separation of variables and integration of Equation (2) assuming constant w, b, c_p, and T₀ yields

$$\frac{H(0.95T_0)}{wbc_p} (t - t_i) = \ln \left[\frac{0.95T_0 - TW_i}{0.95T_0 - TW} \right] \quad (3)$$

Differentiation of Eq. (3) with respect to time gives

$$\frac{H(0.95T_0)}{wbc_p} = \frac{d}{dt} \ln \left[\frac{0.95T_0 - TW_i}{0.95T_0 - TW} \right] \quad (4)$$

Since the left side of Eq. (4) is a constant, plotting $\ln \left[\frac{0.95T_0 - TW_i}{0.95T_0 - TW} \right]$

versus time will give a straight line if conduction is negligible. Thus, deviation from a straight line can be interpreted as conduction effects.

The data were evaluated in this manner, and generally a linear portion of the curve was used for all thermocouples. A linear least-square curve fit of $\ln [(0.95T_0 - TW_i)/(0.95T_0 - TW)]$ versus time was applied to the data. The data reduction time was delayed for all thermocouples that were influenced by the tunnel induced shock until they had cleared this region. The thermocouples on the external tank and both SRB's with an X/L greater than 0.9 were reduced starting 3.9 seconds after centerline. The thermocouples with an X/L greater than 0.2 on the external tank and an X/L greater than 0.113 on each SRB but not exceeding an X/L of 0.9 were reduced starting at 2.6 seconds after centerline. The remaining thermocouples on the external tank and each SRB were reduced starting at centerline. The thermocouples on the orbiter with an X/L greater than 0.055 were reduced starting at 2.6 seconds after centerline. All other thermocouples on the orbiter were reduced starting at centerline. The curve fit extended for a time span which was a function of the heating rate, as shown on the following list.

<u>Range</u>	<u>No. of Points (Fit Length)</u>
$\frac{dT_W}{dt} > 32$	5
$16 < \frac{dT_W}{dt} \leq 32$	7
$8 < \frac{dT_W}{dt} \leq 16$	9
$4 < \frac{dT_W}{dt} \leq 8$	13
$2 < \frac{dT_W}{dt} \leq 4$	17
$1 < \frac{dT_W}{dt} \leq 2$	25
$\frac{dT_W}{dt} \leq 1$	41

The above time spans were adequate to keep the evaluation of the right side of Eq. (4) within the linear region. The linearity of the fit was substantiated by visual inspection of the cases in question. This visual check of the data was done on the VKF graphics terminal. Strictly speaking, the value of c_p for the material was not constant, and the following relation

$$c_p = 0.0797 + (5.556 \times 10^{-5}) TW, \text{ (17-4 PH stainless steel) Btu/lbm}^{\circ}\text{R} \quad (5)$$

was used with the value of TW at the midpoint of the curve fit. The maximum variation of c_p over any curve fit was less than 1.2 percent. The value of density used for 17-4 PH stainless steel was

$$w = 490.0 \text{ lbm/ft}^3$$

3.3 ADIABATIC WALL TEMPERATURE

The maximum available tunnel stagnation temperature for each Mach number tested is listed in Section 3.1. With these relatively low stagnation temperatures, the difference between the model wall temperature and recovery temperature was generally small in regions of peak heating. This small temperature difference causes the calculation of the heat-transfer coefficient to be very sensitive to deviations from the actual adiabatic wall temperature. Two values of the heat-transfer coefficient have been calculated based on an assumed constant recovery temperature, namely $H(T_0)$ and $H(0.95T_0)$. To account for changes in the recovery temperature a third value of the heat-transfer coefficient has been tabulated based on an analytical temperature ratio, $R = T_{AW}/T_0$.

The analytical method for determining R was developed by Rockwell International and has been used to calculate $H(RT_0)$. In this method, the following relationships were assumed:

$$R = \frac{T_{AW}}{T_0} \quad (6)$$

and

$$T_{AW} = T_e \left(1 + \frac{\gamma-1}{2} r M_e^2\right) \quad (7)$$

$$r = 0.898 \text{ for turbulent flow}$$

with r being the recovery factor and the subscript e identifying local properties at the boundary-layer edge. From these relationships, the temperature ratio can be defined as:

$$R = \frac{1 + 0.2 r M_e^2}{1 + 0.2 M_e^2} \quad (8)$$

which is a function of the recovery factor and the local Mach number. The local Mach number can be written

$$M_e = M_e(M_\infty, \delta) \quad (9)$$

where ∞ identifies the free-stream property and δ is the local surface angle of attack.

The local Mach number can be approximated by using tangent cone flow theory, and was used in Equation (8) to give R as a function of M_∞ and δ . Calculations of R were made for several values of M_∞ and δ , and the results were curve fit by Rockwell International. The following equation resulted

$$R(M_\infty, \delta) = a_1 + a_2 \cdot (\sin \delta)^{a_3} \quad (10)$$

where a_1 , a_2 , a_3 are constants for a particular Mach number. The values of a_1 , a_2 , a_3 used for this test are:

M_∞	a_1	a_2	a_3
3.0	0.9345	0.1004	2.165
4.0	0.922	0.1004	1.965

Standard matrix techniques, Ref. 3, were used to derive the following relations for δ , as applicable to the model geometry.

$$\delta = \arcsin (\sin \lambda \cos \alpha_s + \cos \lambda \cos \epsilon \sin \alpha_s), \text{ deg} \quad (11)$$

where

$$\epsilon = \text{roll model} + (\theta + 180), \text{ deg}; \text{ for external tank}$$

$$\epsilon = \text{roll model} + (\psi + 180), \text{ deg}; \text{ for left SRB}$$

$$\epsilon = \text{roll model} + (180 - \psi), \text{ deg}; \text{ for right SRB}$$

Additional information would have been required pertaining to the directional cosines at each thermocouple location to calculate δ on the orbiter. This would be necessary since the orbiter model is not symmetrical about the axial centerline. However, this additional information was not available so a modified approach was selected. The equations for calculating δ for the various thermocouples on the orbiter model are shown in Table 3.

The method used to calculate the analytical temperature ratio, R has been applied to all of the tabulated data. The method represents a simplified approach to present a more realistic evaluation of TAW. However, in regions of separated flow or complex interaction, the values calculated for R may no longer apply and should be used with extreme care.

3.4 UNCERTAINTY OF MEASUREMENTS

3.4.1 Test Conditions

The accuracy of the basic measurements (p_o and T_o) was discussed in Section 2.3. Based on repeat calibrations, these errors were found to be

$$\frac{\Delta p_o}{p_o} = 0.002 = 0.2\%, \quad \frac{\Delta T_o}{T_o} = 0.005 = 0.5\%$$

Uncertainties in the basic tunnel parameters p_o and T_o (see Section 2.3) and the two-sigma deviation in Mach number determined from test section flow calibrations were used to estimate uncertainties in the other free-stream properties, using the Taylor series method of propagation, i. e.

$$(\Delta F)^2 = \left(\frac{\partial F}{\partial X_1} \Delta X_1 \right)^2 + \left(\frac{\partial F}{\partial X_2} \Delta X_2 \right)^2 + \left(\frac{\partial F}{\partial X_3} \Delta X_3 \right)^2 + \dots + \left(\frac{\partial F}{\partial X_n} \Delta X_n \right)^2 \quad (11)$$

where ΔF is the absolute uncertainty in the dependent parameter $F = F(X_1, X_2, X_3 \dots X_n)$ and X_n is the independent parameter (or basic measurement). ΔX_n is the uncertainty (error) in the independent measurement (or variable).

The computed uncertainties in the tunnel free-stream conditions are summarized in the following table.

<u>Uncertainty, (\pm) percent of actual value</u>				
<u>M_∞</u>	<u>M_∞</u>	<u>p_∞</u>	<u>q_∞</u>	<u>RE/FT</u>
3.0	0.6	2.6	1.4	1.2
4.0	0.4	2.4	1.5	1.2

The uncertainty in model angle of attack (ALPHA-MODEL), as determined from tunnel sector calibration and consideration for possible sting deflections, is estimated to be ± 0.5 deg.

3.4.2 Test Data

Estimated uncertainties in w , b , c in Eq. (2) combined with computed uncertainties for $(dT_w/dt)/(0.95T_o - T_w)$ in the Taylor series method of error

propagation gave the following uncertainties in the heat-transfer coefficient for the listed range of values:

$H(0.95T_0)$, <u>Btu</u> <u>ft²-sec°R</u>	<u>Uncertainty, percent(±)</u>
10^{-2}	9.5
10^{-3}	11
10^{-4}	12

The data were deleted from the results for thermocouples which consistently exceeded the above quoted uncertainties.

4.0 DATA PACKAGE PRESENTATION

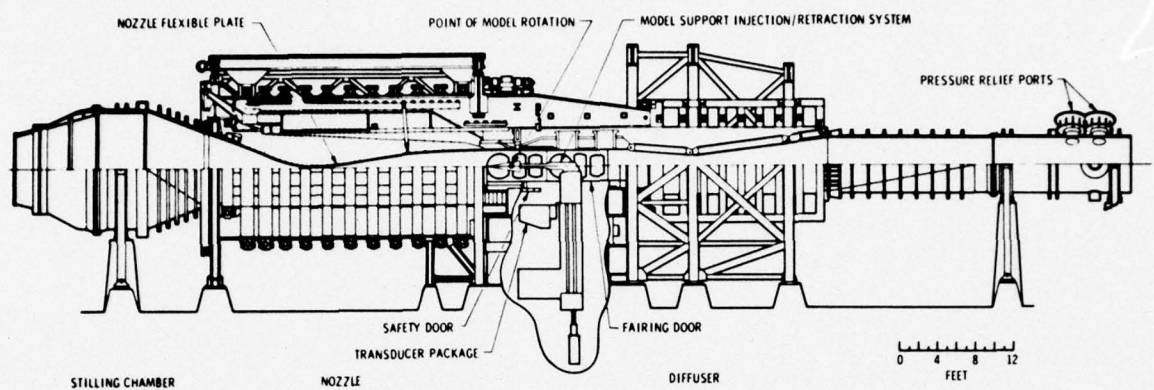
Convective heat-transfer-rate distributions were obtained on a 0.0175-scale model of the Space Shuttle Integrated Model. Typical data tabulations are illustrated in Fig. 5. The final tabulated data were transmitted with this report to NASA-JSC and Rockwell International.

Representative data from the top centerline of the external tank ($\theta = 0$ deg) are presented for a free stream Mach number of 3.01 and 4.02 in Figs. 6 and 7, respectively. These data were obtained with the model in the OTS configuration. The location of the orbiter nose and each SRB nose is located on each figure in terms of the X/L for the external tank. The theoretical data for each Mach number is based on the external tank alone with no protuberances. The theoretical data were derived by using calculations described in Refs. 4 and 5. In general, the data are in good agreement with the theoretical values on the ogive section of the external tank at both Mach numbers. In this region the flow is not disturbed by the other model components and closely approximates the assumptions stated for the theoretical calculations. The trend toward the junction of the nose ogive with the cylindrical body has been consistently observed on the external tank but is not adequately predicted by the theory. The data agreement with the data from a previous test, (IH-72) is generally very good for both Mach numbers. The agreement with theoretical heat-transfer-rates and with previous data is considered as adequate for validation of the basic test results.

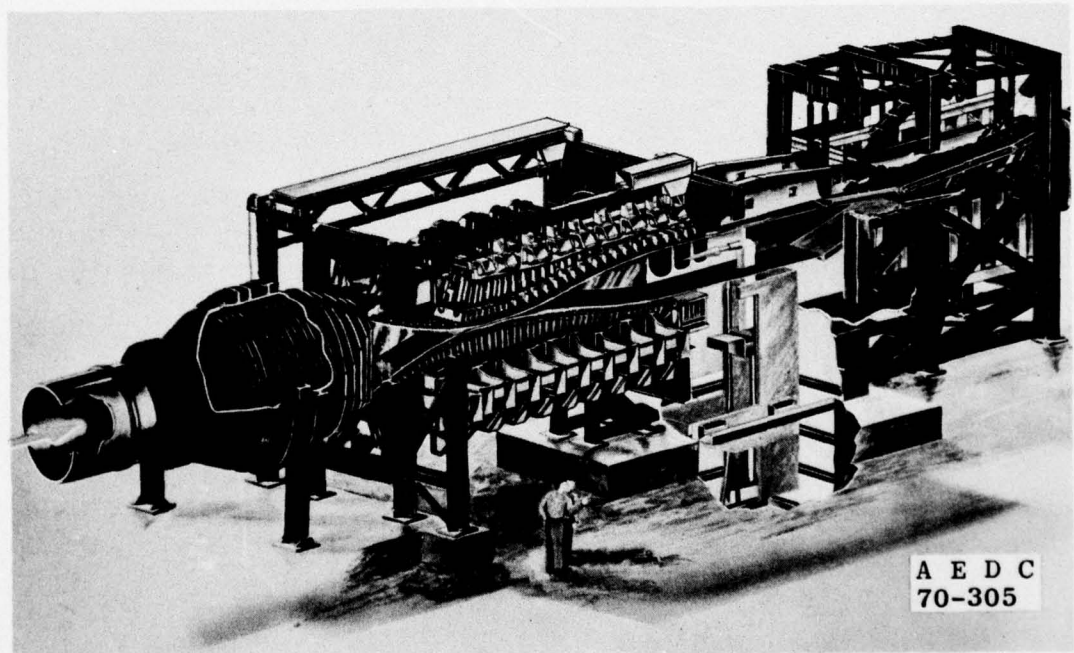
REFERENCES

1. Test Facilities Handbook (Tenth Edition) "von Karman Gas Dynamics Facility," Arnold Engineering Development Center, May 1974.
2. Hilsch, R. "The Use of the Expansion of Gases in a Centerifugal Field as a Cooling Process." The Review of Scientific Instruments, Vol. 18, No. 2, February 1947.
3. Trimmer, L. L. and Clark, E. L. "Transformation of Axes Systems by Matrix Methods and Applications to Wind Tunnel Data Reduction." AEDC-TDR-63-224, October 1963.
4. DeJarnette, Fred R. "Calculation of Inviscid Surface Streamlines on Shuttle-Type Configurations, Part I - Description of Basic Method." NASA CR-111921, August 1971.
5. DeJarnette, Fred R. and Jones, Michael H. "Calculation of Inviscid Surface Streamlines and Heat Transfer on Shuttle Type Configurations, Part 2 - Description of Computer Program." NASA CR-111922, August 1971.

APPENDIX A
ILLUSTRATIONS



a. Tunnel assembly



b. Tunnel test section
Fig. 1 Tunnel A

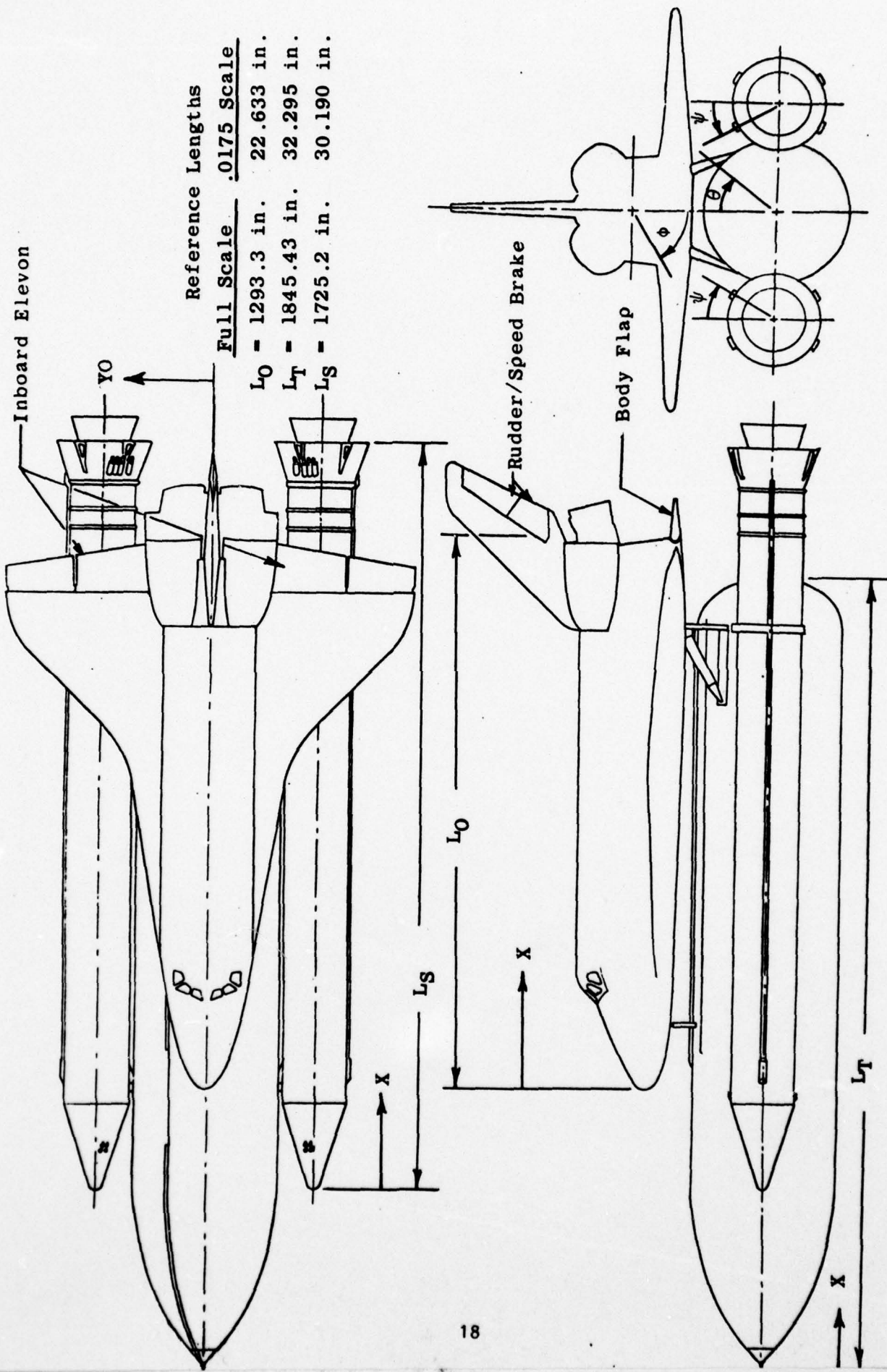


Figure 2. Sketch of the Space Shuttle Integrated Model

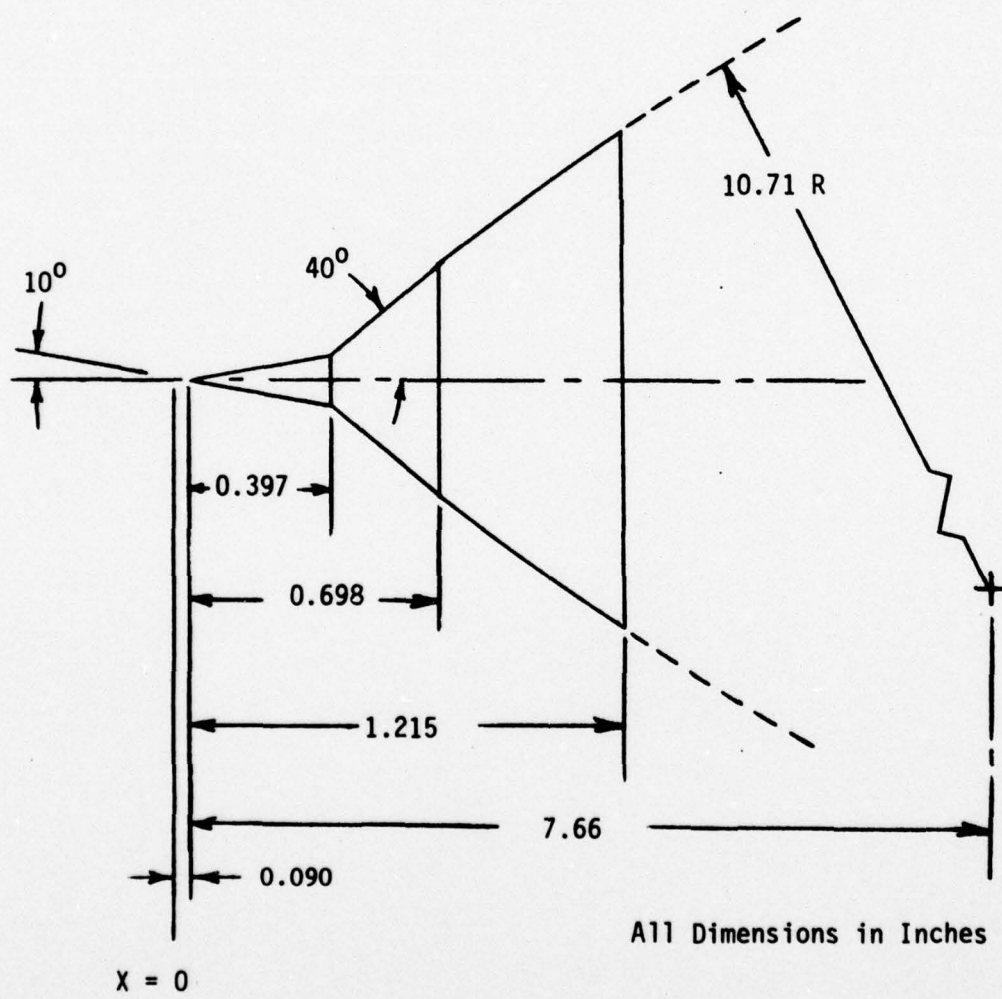


Fig. 3 External Tank Nose Tip Configuration

40-INCH SUPERSONIC TUNNEL A

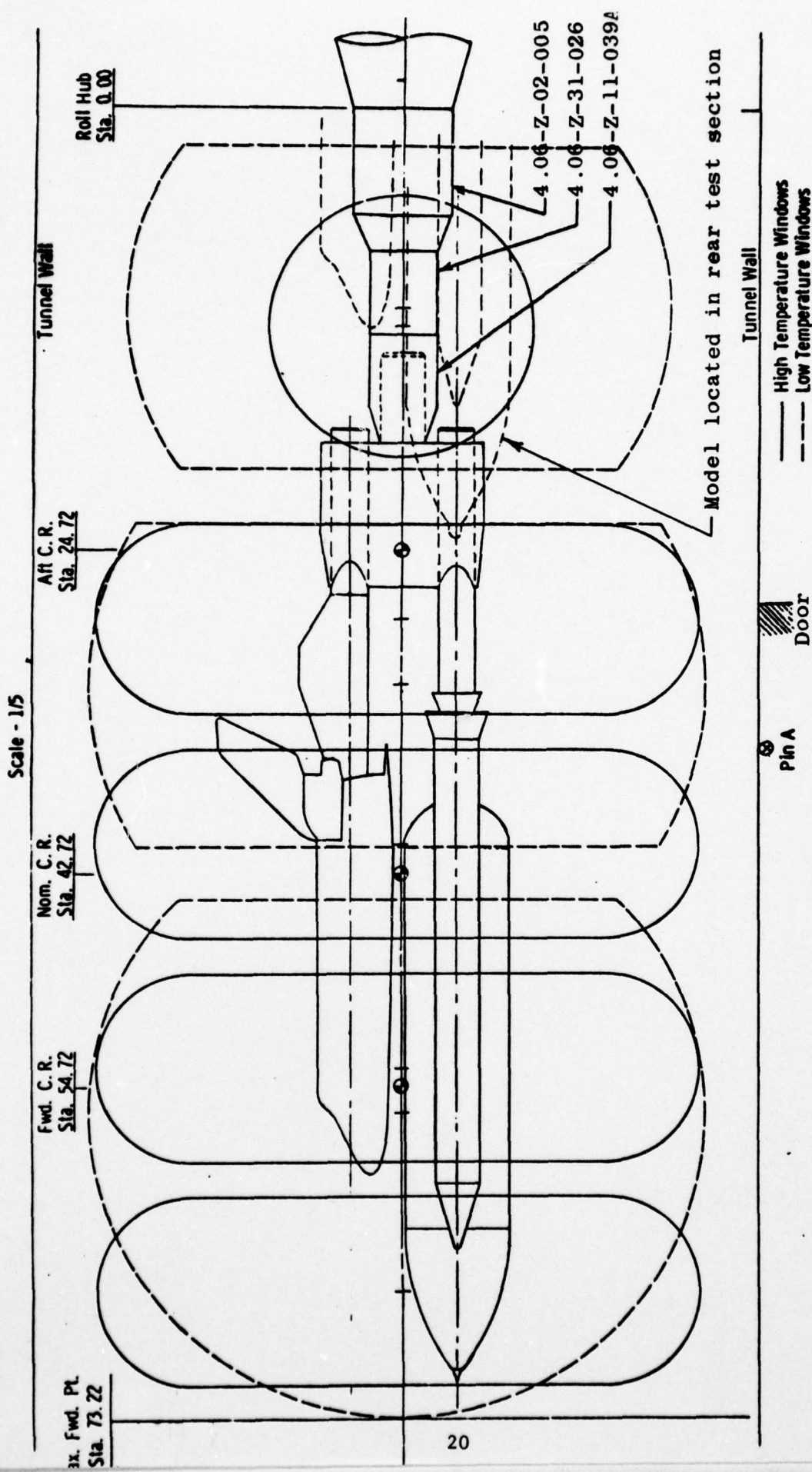


Figure 4. Model Installation in Tunnel A

ARU, INC. - AEDC DIVISION
A STEPHENSON COMPUMATION COMPANY
VON KARMAN GAS DYNAMICS FACILITY
ARNOLD AIR FORCE STATION, TENNESSEE
NASAVRI INHUS HEATING TEST

DATE COMPUTED 14-APR-78
TIME COMPUTED 23:36:40
DATE RECORDED 19-APR-78
TIME RECORDED 23:36:11
PROJECT NUMBER V61A-US

GROUP	COMBUSTANT	MODEL	MACH NO	PU-PSIA	TO,DEG K	ALPHA-MODEL	ALPHA-PREBEND	ROLL-MODEL	YAW
3	SET 211	OTS	3.01	36.9	714.7	0.02	0.02	-0.06	0.00
T-1INF	P=INF	U=INF	RHO=INF	RHO=INF	HT/T	HKEF-FN	HTFK	X/L	THETA
(DEGM)	(PSIA)	(PSIA)	(FT-SEC)	(LB/MFT3)	(FT-1)	(IN U.0175FT)	(IN U.0175FT)		
254.15	0.99	6.269	2354.	1.050E-02	3.770E+06	5.54E-02	9.353E-03	1	
INBOARD	DELTAE	DELTAF	VELTASB						
10.	0.	0.							
TC-NO	T _w	DiagUT	WUT	H(TO)	H(TU)/HREF	H(.95TU)	H(.95TU)/HREF	R	EXT. TANK
2089	6.01.1	11.2d7	1.659	0.146E-01	0.263E-01	0.213E-01	0.384E-01	0.9345	0.248E-01
2088	6.02.4	14.389	2.094	0.187E-01	0.337E-01	0.274E-01	0.494E-01	0.9345	0.320E-01
2087	6.11.2	1.668	0.242	0.249E-02	0.449	0.393E-02	0.709	0.9345	0.478E-02
2089	557.2	5.763	0.880	0.559E-02	0.109	0.723E-02	0.130E	0.9345	0.795E-02
2091	552.0	5.443	0.619	0.512E-02	0.924	0.656E-02	0.924	0.9345	0.720E-02
2092	549.3	5.379	0.619	0.495E-02	0.894	0.632E-02	0.114E	0.9345	0.691E-02
2093	535.5	4.246	0.641	0.358E-02	0.647	0.447E-02	0.608	0.9345	0.495E-02
2094	551.0	5.969	0.211	0.578E-02	0.104E	0.749E-02	0.1351	0.9345	0.823E-02
2095	547.4	7.719	0.869	0.520E-02	0.931E	0.661E-02	0.1193	0.9345	0.722E-02
2096	546.3	4.504	6.618	0.366E-02	0.661	0.453E-02	0.681E	0.9345	0.489E-02
2097	546.4	3.6333	0.546	0.289E-02	0.923	0.357E-02	0.645	0.9345	0.385E-02
2098	DELIE								
2100	DELETE								
2101	526.6	3.993	0.601	0.323E-02	0.584	0.400E-02	0.0722	0.9345	0.432E-02
2102	526.8	4.143	0.627	0.338E-02	0.610	0.419E-02	0.0755	0.9345	0.451E-02
2104	DELETE								
2105	56.7	7.616	1.218	0.802E-02	0.144E	0.105E-01	0.1893	0.9345	0.116E-01
2106	DELETE								
2107	575.1	8.308	1.337	0.958E-02	0.1730	0.129E-01	0.2326	0.9345	0.144E-01
2109	571.1	6.806	1.414	0.985E-02	0.1779	0.131E-01	0.2368	0.9345	0.146E-01
2109	574.4	7.954	1.280	0.912E-02	0.1649	0.122E-01	0.2211	0.9345	0.137E-01
2110	571.2	7.650	1.229	0.857E-02	0.1547	0.114E-01	0.2060	0.9345	0.127E-01
2111	554.6	6.577	1.045	0.653E-02	0.1179	0.849E-02	0.1517	0.9345	0.922E-02
2112	531.8	0.020	0.003	0.182E-04	0.003	0.226E-04	0.0004	0.9345	0.245E-04
2113	567.3	3.342	0.554	0.376E-02	0.679	0.496E-02	0.0896	0.9345	0.551E-02
2114	571.0	3.512	0.593	0.406E-02	0.753	0.541E-02	0.0976	0.9345	0.602E-02
2115	575.0	3.158	0.521	0.373E-02	0.674	0.502E-02	0.0906	0.9345	0.561E-02
2116	565.4	3.227	0.531	0.356E-02	0.663	0.464E-02	0.0845	0.9345	0.518E-02
2117	DELETE								
2118	570.1	3.949	0.654	0.452E-02	0.0017	0.601E-02	0.1085	0.9345	0.669E-02

NOTE: THIS IS A TYPICAL PAGE FROM A MULTIPLE PAGE TABULATION

Figure 5. Typical Heat-Transfer Data Tabulation

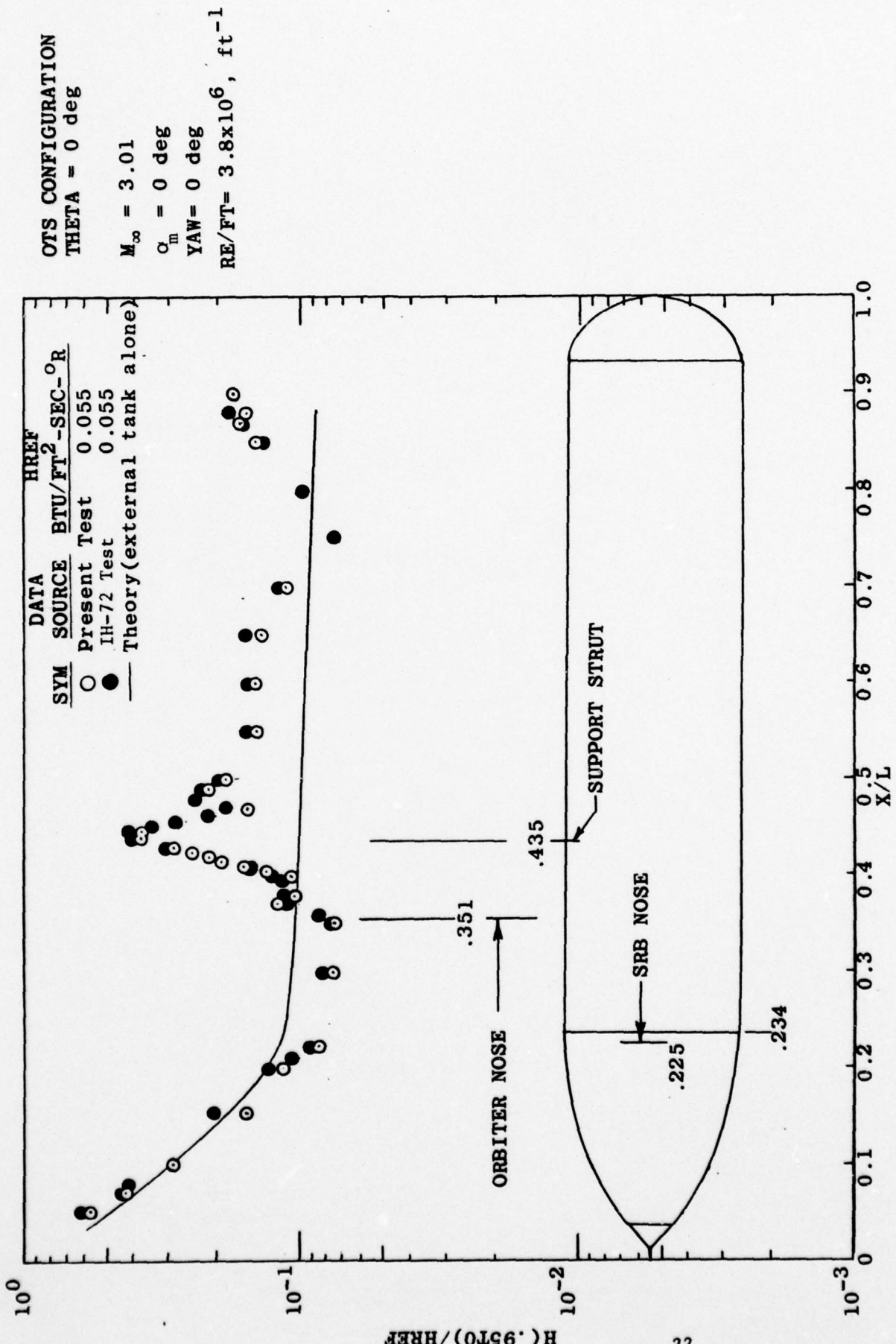


Figure 6. Comparison of External Tank Data for the OTS Configuration with Theory and Results from a Previous Test at Mach 3.01

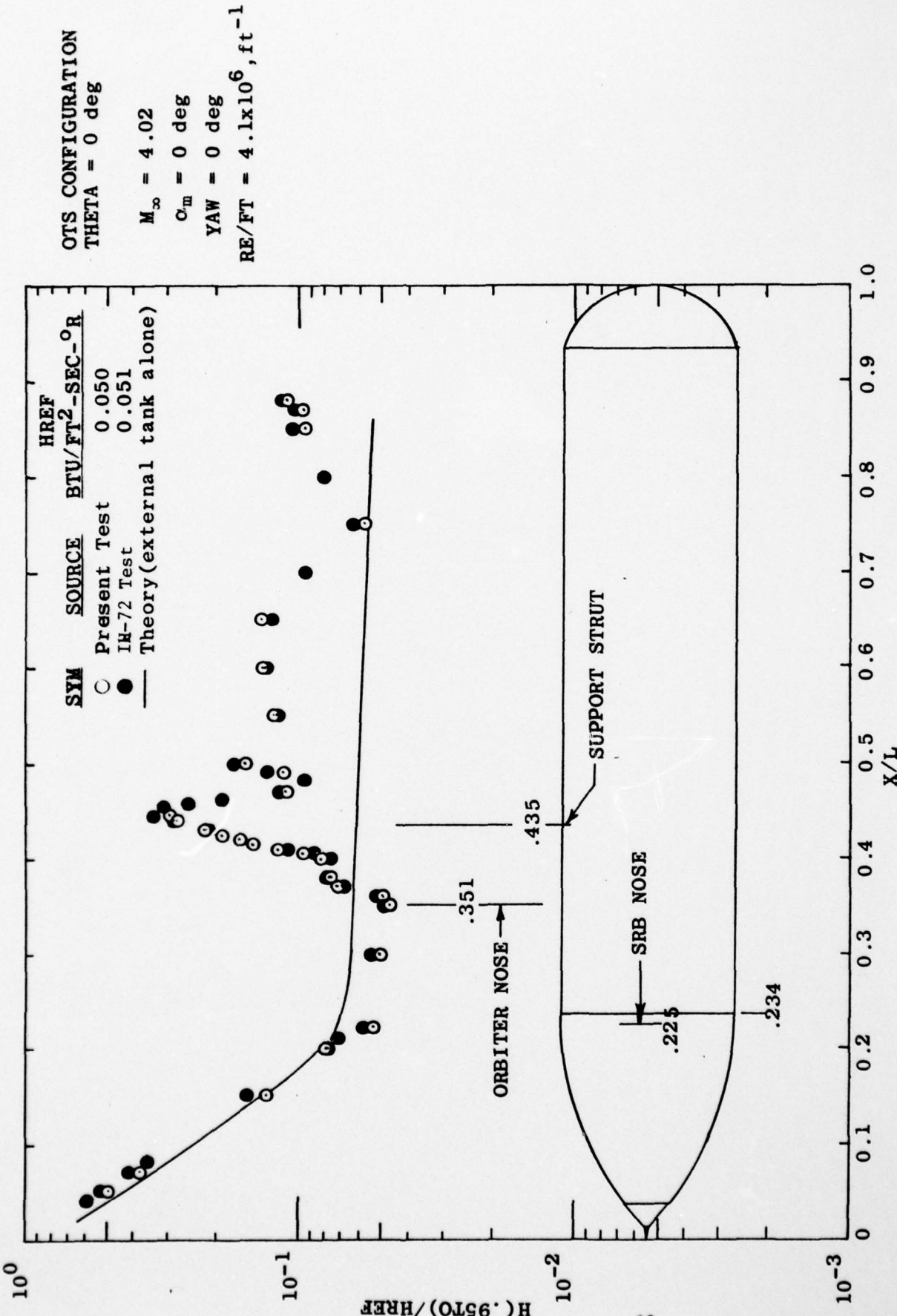


Figure 7. Comparison of External Tank Data for the OTS Configuration with Theory and Results from a Previous Test at Mach 4.02

APPENDIX B

TABLES

TABLE 1. THERMOCOUPLE CONSTANT SETS
EXTERNAL TANK

CONSTANT SET 111

Ch. No.	T/C	X/L	θ	Ch. No.	T/C	X/L	θ	Ch. No.	T/C	X/L	θ
1	615	.38	0	34	649	.95	0	66	696	.926	17
2	616	.385		35	650	.35	11.25	67	OPEN		
3	617	.39		36	651	.36		68	OPEN		
4	618	.395		37	652	.37		69	699	.05	29.8
5	619	.40		38	653	.375		70	700	.07	
6	620	.405		39	654	.38		71	701	.10	
7	621	.41		40	655	.385		72	702	.15	
8	622	.415		41	656	.39		73	703	.20	
9	623	.42		42	657	.395		74	704	.30	
10	624	.425		43	658	.40		75	705	.35	
11	625	.43		44	659	.405		76	706	.375	
12	626	.44		45	660	.41		77	707	.50	
13	627	.445		46	676	.85		78	708	.60	
14	628	.45		47	677	.86		79	709	.70	
15	629	.455		48	678	.87		80	710	.80	
16	630	.46		49	679	.88		81	711	.87	
17	631	.47		50	680	.89		82	712	.926	↓
18	632	.48		51	681	.90		83	OPEN		
19	633	.49		52	682	.91		84	OPEN		
20	634	.50		53	683	.926	↓	85	715	.05	37.7
21	635	.55		54	684	.95	↓	86	716	.07	
22	636	.60		55	685	.33	17	87	717	.10	
23	637	.65		56	686	.34		88	718	.15	
24	638	.70		57	687	.35		89	719	.20	
25	639	.75		58	688	.36		90	720	.30	
26	640	.80		59	689	.37		91	721	.35	
27	641	.85		60	690	.375		92	722	.375	
28	642	.86		61	691	.50		93	723	.50	
29	643	.87		62	692	.60		94	724	.60	
30	644	.88		63	693	.70		95	725	.70	
31	645	.89		64	694	.80		96	726	.80	
32	646	.90		65	695	.87	↓	97	727	.87	↓
33	648	.926	↓								

TABLE 1. Continued
EXTERNAL TANK

CONSTANT SET 122

Ch. No.	T/C	X/L	θ
1	728	.926	37.7
2	OPEN		
3	OPEN		
4	2181	.01	180
5	2182	.015	
6	2183	.02	
7	2184	.025	
8	2185	.03	↓
9	843	.30	292.5
10	844	.33	
11	845	.35	
12	846	.37	
13	847	.40	
14	848	.45	
15	849	.50	
16	850	.55	
17	851	.60	
18	852	.65	
19	853	.70	
20	854	.75	
21	855	.80	
22	856	.90	↓
23	857	.84	305.4
24	858	.85	
25	859	.86	
26	860	.87	
27	861	.88	
28	862	.89	
29	863	.90	
30	864	.91	
31	865	.926	↓
32	866	.80	309.3
33	867	.81	↓

Ch. No.	T/C	X/L	θ
34	868	.82	309.3
35	869	.83	↓
36	870	.04	315
37	871	.05	
38	872	.06	
39	888	.85	
40	889	.86	
41	890	.87	
42	891	.88	
43	892	.89	
44	893	.90	
45	894	.91	
46	895	.926	
47	896	.95	↓
48	897	.42	322.3
49	898	.435	
50	899	.45	
51	900	.50	
52	901	.60	
53	902	.70	
54	903	.80	
55	904	.87	↓
56	905	.42	330.2
57	906	.435	
58	907	.45	
59	908	.50	
60	909	.60	
61	910	.70	
62	911	.80	
63	912	.87	
64	913	.935	
65	914	.945	↓

Ch. No.	T/C	X/L	θ
66	915	.04	337.5
67	916	.05	
68	917	.06	
69	918	.07	
70	919	.08	
71	920	.10	
72	921	.15	
73	922	.20	
74	923	.42	
75	924	.435	
76	925	.45	
77	926	.85	
78	927	.86	
79	928	.87	
80	929	.88	
81	930	.89	
82	931	.90	
83	932	.91	↓
84	963	.455	348
85	964	.46	
86	965	.47	
87	966	.48	
88	967	.49	
89	968	.85	
90	969	.86	
91	970	.87	
92	971	.88	
93	972	.89	
94	973	.90	
95	974	.91	
96	975	.926	
97	976	.95	↓

TABLE 1. Continued
EXTERNAL TANK

CONSTANT SET 133

Ch. No.	T/C	X/L	θ	Ch. No.	T/C	X/L	θ	Ch. No.	T/C	X/L	θ
1	2186	.02	0	34	2014	.686	31.43	66	2046	.44	45
2	2187	.025		35	2015	.720		67	2047	.45	
3	2188	.03	↓	36	2016	.756		68	2048	.47	
4	985	.04	270	37	2017	.790		69	2049	.55	
5	986	.05		38	2018	.825		70	2050	.60	
6	987	.06		39	2019	.860		71	2051	.65	
7	988	.07		40	2020	.895	↓	72	2052	.75	
8	989	.08		41	2021	.441	326.9	73	2053	.80	
9	990	.10		42	2022	.476		74	2054	.83	
10	991	.15		43	2023	.511		75	2055	.84	
11	992	.20	↓	44	2024	.547		76	2056	.85	
12	993	.01	39	45	2025	.582		77	2057	.86	
13	994	.025	↓	46	2026	.617		78	2058	.87	
14	OPEN			47	2027	.652		79	2059	.88	
15	995	.03	39	48	2028	.687		80	2060	.89	
16	OPEN			49	2029	.723		81	2061	.90	
17	OPEN			50	2030	.758		82	2062	.91	
18	OPEN			51	2031	.793		83	2063	.926	
19	2000	.435	23.07	52	2032	.828		84	2064	.935	
20	2001	.569		53	2033	.864		85	2065	.945	↓
21	2002	.703		54	2034	.899		86	2066	.25	36.32
22	2003	.836		55	2035	.934	↓	87	2067	.30	
23	2004	.899	↓	56	2036	.250	45	88	2068	.325	
24	OPEN			57	2037	.300		89	2069	.35	
25	2005	.476	31.43	58	2038	.325		90	2070	.375	
26	2006	.511		59	2039	.350		91	2071	.40	↓
27	2007	.546		60	2040	.375		92			
28	2008	.581		61	2041	.400		93			
29	2009	.616		62	2042	.420		94			
30	2010	.651	↓	63	2043	.425		95			
31	OPEN			64	2044	.430		96			
32	OPEN			65	2045	.435	↓	97			
33	OPEN										

TABLE 1. Continued
EXTERNAL TANK

CONSTANT SET 211

Ch. No.	T/C	X/L	θ	Ch. No.	T/C	X/L	θ	Ch. No.	T/C	X/L	θ
1	2089	.937	352.2	34	2120	.85	301.5	66	2152	.926	33.75
2	2088		289.4	35	2121	.86		67	2153		31.75
3	2087		250.6	36	2122	.87		68	2154		23.07
4	2090	.355	29.8	37	2123	.88		69	OPEN		
5	2091	.360		38	2124	.89		70	OPEN		
6	2092	.365		39	2125	.90		71	OPEN		
7	2093	.370		40	OPEN			72	2158	.926	355.2
8	2094	.355	23.08	41	2127	.925	301.5	73	OPEN		
9	2095	.360		42	2128	.935		74	2160	.926	345.2
10	2096	.365		43	2129	.82	292	75	2161		335
11	2097	.370		44	2130	.83		76	2162		330.2
12	2098	.355	20.98	45	2131	.84		77	2163		326.9
13	2099	.360		46	2132	.85		78	2164		324.5
14	2100	.365		47	2133	.86		79	OPEN		
15	2101	.370		48	2134	.87		80	2166	.441	31.43
16	2102	.355	17.0	49	2135	.88		81	2167	.425	337.5
17	OPEN			50	2136	.89		82	2168		345.6
18	2104	.400	330.2	51	2137	.91		83	2169		354
19	2105	.405		52	2138	.926		84	2170		5.68
20	2106	.410		53	2139	.93		85	2171		17
21	2107	.400	326.8	54	2140	.926	299.4	86	2172	.430	337.5
22	2108	.405		55	2141		270	87	2173		345.6
23	2109	.405	324.5	56	2142		258	88	2174		354
24	2110	.410		57	2143		250.6	89	2175		5.68
25	2111	.410	315	58	2144		247.5	90	2176		17
26	2112	.835	309.3	59	2145	.93	289.4	91	600	.04	0
27	2113	.820	305.4	60	2146		270	92	601	.05	
28	2114	.830		61	2147		258	93	602	.06	
29	2115	.835		62	2148		250.6	94	603	.07	
30	2116	.820	301.5	63	2149		247.5	95	604	.08	
31	2117	.830		64	2150	.935	270	96	605	.10	
32	2118	.835		65	2151		258	97	606	.15	
33	2119	.840									

TABLE 1. Continued
EXTERNAL TANK AND RIGHT SRB
CONSTANT SET 222

Ch. No.	T/C	X/L	θ/ψ^*	Ch. No.	T/C	X/L	ψ	Ch. No.	T/C	X/L	ψ
1	607	.20	0	34	1524	.967	225	66	1556	.985	355
2	608	.21		35	1525	.953	216	67	1557	.964	330.7
3	609	.22		36	1526	.965	217	68	1558	.978	↓
4	610	.30		37	1527	.975	218	69	1559	.982	320
5	611	.35		38	1528	.985	219	70	1560	.954	324
6	612	.36		39	1529	.995	220	71	1561	.975	↓
7	613	.37		40	1530	.954	210	72	1562	.954	336
8	614	.375	↓	41	1531	.953	156	73	1563	.982	334
9	1478	.937	263	42	1532	.967	157	74	1564	.975	336
10	1500	.953	0	43	1533	.980	158	75	1565	.982	340
11	1501	.965		44	1534	.994	159	76	1566	.954	342
12	1502	.975		45	1535	.953	204	77	1567	.964	↓
13	1503	.985		46	1536	.967	203	78	1568	.975	↓
14	1504	.995	↓	47	1537	.980	202	79	1569	.982	350
15	1505	.953	24	48	1538	.994	201	80	1570	.975	353
16	1506	.967	23	49	1539	.954	210	81	OPEN		
17	1507	.980	22	50	1540	.953	216	82	OPEN		
18	1508	.994	21	51	1541	.967	217	83	OPEN		
19	1509	.954	30	52	1542	.980	218	84	1574	.971	11
20	1510	.953	36	53	1543	.994	219	85	1575	.978	11
21	1511	.967	323	54	1544	.953	320	86			
22	1512	.980	322	55	1545	.965	↓	87			
23	1513	.994	321	56	1546	.985	↓	88			
24	1514	.953	315	57	1547	.975	322.5	89			
25	1515	.953	306	58	1548	.985	↓	90			
26	1516	.967	308	59	1549	.954	330	91			
27	1517	.980		60	1550	.995	340	92			
28	1518	.994	↓	61	1551	.985	345	93			
29	1519	.953	234	62	1552	.995	↓	94			
30	1520	.965	230	63	1553	.985	350	95			
31	1521	.975		64	1554	.995	↓	96			
32	1522	.985	↓	65	1555	.953	355	97			
33	1523	.953	225								

* θ Applies through Channel 8, ψ starts with Channel 9

TABLE 1. Continued
ORBITER

CONSTANT SET 233

Ch. No.	T/C	X/L	ϕ	Ch. No.	T/C	X/L	ϕ	Ch. No.	T/C	X/L	ϕ
1	OPEN			34	301	.843		66	338	1.01	
2	227	.60	157.5	35	302	.862		67	339	↓	
3	228	.65		36	OPEN			68	OPEN		
4	229	.70		37	304	.862		69	183	.45	180
5	230	.75	↓	38	305		↓	70	185	.55	
6	234	.40	135	39	306		↓	71	187	.65	↓
7	238	.60		40	308	.881		72	OPEN		
8	239	.65		41	309		↓	73	190	.80	180
9	240	.70		42	310		↓	74	506	.868	--
10	241	.75		43	311		↓	75	509	.847	
11	242	.80	↓	44	OPEN			76	515	.839	
12	392	.60	114	45	312	.881		77	521	.858	
13	393	.65		46	315	.920		78	522	.870	
14	394	.70		47	316		↓	79	523	.837	
15	395	.75		48	317		↓	80	527	.861	
16	OPEN			49	318		↓	81	534	.830	
17	7	.05	0	50	319		↓	82	538	.868	
18	8	.06		51	320	.939		83	542	.833	
19	9	.07		52	321		↓	84	20	.19	0
20	10	.08		53	322		↓	85	21	.20	
21	11	.09		54	323		↓	86	23	.25	
22	12	.10	↓	55	325		↓	87	24	.30	
23	207	.10	20	56	327	.978		88	25	.35	
24	208	.10	24.5	57	328		↓	89	26	.40	
25	13	.12	0	58	329		↓	90	27	.45	
26	14	.13		59	330		↓	91	28	.50	
27	15	.14		60	331		↓	92	29	.55	
28	16	.15		61	332	.997		93	OPEN		
29	17	.16		62	333		↓	94	32	.70	
30	18	.17		63	334		↓	95	33	.75	
31	19	.18	↓	64	335		↓	96	36	.90	↓
32	299	.843		65	337	1.01		97			
33	300	.843									

TABLE 1. Continued
LEFT SRB

CONSTANT SET 311

Ch. No.	T/C	X/L	ψ	Ch. No.	T/C	X/L	ψ	Ch. No.	T/C	X/L	ψ
1	1000	.115	0	34	1033	.925	45	66	1065	.115	135
2	1001	.20		35	1034	.953	50	67	1066	.143	
3	1002	.225		36	1035	.967		68	1067	.171	
4	1003	.25		37	1036	.980		69	1068	.20	
5	1004	.30		38	1037	.994		70	1069	.30	
6	1005	.40		39	1038	0	90	71	1070	.50	
7	1006	.50		40	1039	.002		72	1071	.60	
8	1007	.55		41	1040	.008		73	1072	.70	
9	1008	.60		42	1041	.050		74	1073	.80	
10	1009	.65		43	1042	.10		75	1074	.953	
11	1010	.70		44	1043	.12		76	1124	.177	315
12	1011	.75		45	1044	.127		77	1125	.20	
13	1012	.80		46	1045	.134		78	1126	.30	
14	1013	.875		47	1046	.173		79	1127	.50	
15	1014	.925		48	1047	.180		80	1128	.60	
16	1015	.939		49	1048	.186		81	1129	.70	
17	1016	.953	355	50	1049	.193		82	1130	.80	
18	1017	.967		51	1050	.20		83	1131	.875	
19	1018	.980		52	1051	.25		84	1132	.925	
20	1019	.994		53	1052	.30		85	1133	.953	
21	1020	.115	45	54	1053	.40		86	1134	.967	
22	1021	.143		55	1054	.50		87	1135	.980	
23	1022	.171		56	1055	.60		88	1136	.994	
24	1023	.20		57	1056	.70		89	1200	.043	65
25	1024	.30		58	1057	.75		90	1201	.05	
26	1025	.40		59	1058	.80		91	1202	.057	
27	1026	.50		60	1059	.875		92	1203	.063	
28	1027	.55		61	1060	.925		93	1204	.090	
29	1028	.60		62	1061	.953		94	1205	.10	
30	1029	.65		63	1062	.967		95	1206	.05	35
31	1030	.70		64	1063	.980		96	1207	.09	
32	1031	.80		65	1064	.994		97	1208	.10	
33	1032	.875									

TABLE 1. Continued
LEFT AND RIGHT SRB *

CONSTANT SET 322

Ch. No.	T/C	X/L	ψ
1	1209	.05	5
2	1210	.09	
3	1211	.10	↓
4	1212	.043	335
5	1213	.05	
6	1214	.057	
7	1215	.063	
8	1216	.090	
9	1217	.10	↓
10	1220	.965	4.38
11	1221	.975	
12	1222	.985	
13	1223	.995	↓
14	1224	.965	20
15	1225	.975	
16	1226	.985	
17	1227	.995	↓
18	1228	.965	40
19	1229	.975	
20	1230	.985	
21	1231	.995	↓
22	1232	.724	0
23	1233	.724	225
24	OPEN		
25	1235	.724	315
26	1236		330
27	1237	↓	135
28	1238	.74	180
29	1239	↓	225
30	OPEN		
31	1241	.74	315
32	1242		0
33	1243	↓	135

Ch. No.	T/C	X/L	ψ
34	1244	.75	225
35	1245		315
36	1246	↓	135
37	1247	.771	180
38	1248	↓	225
39	OPEN		
40	1250	.771	315
41	1251		0
42	1252	↓	135
43	1253	.932	180
44	1254	↓	225
45	OPEN		
46	1256	.932	315
47	1257		0
48	1258		45
49	1259	↓	135
50	1260	.939	180
51	1261	↓	225
52	OPEN		
53	1263	.939	315
54	1264		45
55	1265	↓	135
56	1266	.953	138
57	1267	↓	162
58	1268	.967	138
59	1269	↓	162
60	1270	.98	138
61	1271	↓	162
62	1272	.994	138
63	1273	↓	162
64	1274	.953	302
65	1275	↓	342

Ch. No.	T/C	X/L	ψ
66	1276	.953	198
67	1277		238
68	1278	.967	302
69	1279		342
70	1280		198
71	1281		238
72	1282	.98	302
73	1283		342
74	1284		198
75	1285		238
76	1286	.994	302
77	1287		342
78	1288		198
79	1289	↓	238
80	1290	.12	76
81	1291	.127	
82	1292	.134	
83	1293	.173	
84	1300	.025	180
85	1302	.075	↓
86	1305	.025	270
87	1307	.075	↓
88	1311	.025	0
89	1313	.075	5
90	1314	.110	5
91	1316	.075	20
92	1317	.090	20
93	1318	.100	
94	1319	.110	↓
95	1321	.075	35
96	1322	.110	↓
97	1323	.110	65

* Thermocouples on the LEFT SRB (Channels 1-83), RIGHT SRB (Channels 84-97)

TABLE 1. Continued *
LEFT AND RIGHT SRB

CONSTANT SET 333

Ch. No.	T/C	X/L	ψ	Ch. No.	T/C	X/L	ψ	Ch. No.	T/C	X/L	ψ
1	1324	.10	76	34	1383	.74	67.5	66	1418	.750	112.5
2	1326	.025	90	35	1384	.75	↓	67	1420	.925	
3	1328	.06		36	1386	.141	76	68	1421	.932	
4	1329	.075	↓	37	1387	.148		69	1422	.939	↓
5	1330	.10	104	38	1388	.155		70	1423	.40	135
6	1332	.025	135	39	1389	.162		71	1425	.98	225
7	1334	.075		40	1390	.25	↓	72	1426	.994	↓
8	1335	.10	↓	41	1393	.74	90	73	1430	.953	4.25
9	1336	.136	263	42	1394	.765		74	1431		15.6
10	1344	.939	↓	43	1395	.771		75	1432		20
11	1345	.115	270	44	1396	.815		76	1433		24.4
12	1346	.136	277	45	1397	.837		77	1434		35.6
13	1347	.30		46	1398	.884		78	1435		40
14	1348	.75		47	1399	.894		79	1436		77.5
15	1349	.815		48	1400	.907		80	1437	.967	
16	1350	.837		49	1401	.917		81	1438	.98	
17	1351	.884		50	1402	.932		82	1439	.994	↓
18	1352	.894		51	1403	.939	↓	83	1440	.953	112.5
19	1354	.939	↓	52	1404	.120	104	84	1441	.967	
20	1355	.74	337.5	53	1405	.127		85	1442	.98	
21	1356	.75	↓	54	1406	.134		86	1443	.994	↓
22	1362	.765	0	55	1407	.141		87	1444	FWD	SEP
23	1363	.815		56	1408	.148		88	1445	MOTORS	
24	1364	.837		57	1409	.155		89	1446		
25	1365	.884		58	1410	.162		90	1447		
26	1366	.907	↓	59	1411	.173		91	1448		↓
27	1368	.74	22.5	60	1412	.180		92	1294	.18	76
28	1369	.75		61	1413	.186		93	1295	.186	
29	1372	.925		62	1414	.193		94	1296	.193	
30	1373	.932		63	1415	.200		95	1297	.20	↓
31	1374	.939	↓	64	1416	.250	↓	96			
32	1375	.74	45	65	1417	.740	112.5	97			
33	1376	.75	↓								

* Thermocouples on the RIGHT SRB (Channels 1-91), LEFT SRB (Channels 92-95)

TABLE 1. Continued
RIGHT SRB

CONSTANT SET 411

Ch. No.	T/C	X/L	ψ
1	1449	FWD.	SEP.
2	1450	MOTORS	
3	1451		
4	1452		
5	1453		
6	1454		
7	1455		
8	1456		
9	1457		
10	1458		
11	1459		
12	1460		
13	1461		
14	1462		
15	1463	.2	277
16	1464	.4	
17	1465	.5	
18	1466	.6	
19	1467	.7	
20	1468	.9	
21	1469	.921	
22	1470	.928	
23	1471	.937	
24	1477	.928	263
25	1479		90
26	1480		
27	1481		
28	1482		
29	1483		
30	1484		
31	1485		
32	1486		
33	1487		

Ch. No.	T/C	X/L	ψ
34	1488		95
35	1489		112
36	1490		
37	1491		
38	1492		
39	1493		
40	1494		140
41	1495		
42	1496		
43	1497		
44	1498		
45	1499		150
46	1298	.008	180
47	1299	.015	
48	1301	.05	
49	1303	.10	
50	1304	.008	270
51	1306	.05	
52	1308	.10	
53	1309	.11	335
54	1310	.008	0
55	1325	.015	90
56	1327	.04	
57	1331	.008	135
58	1333	.05	
59	1337	.30	263
60	1338	.75	
61	1339	.815	
62	1340	.837	
63	1341	.884	
64	1342	.894	
65	1343	.907	

Ch. No.	T/C	X/L	ψ
66	1353	.907	277
67	1357	.765	337.5
68	1358	.771	
69	1359	.925	
70	1360	.932	
71	1361	.939	
72	1367	.724	22.5
73	1370	.765	
74	1371	.771	
75	1377	.765	45
76	1378	.771	
77	1379	.815	
78	1380	.837	
79	1381	.884	
80	1382	.907	
81	1385	.771	67.5
82	1391	.55	90
83	1392	.65	
84	1419	.771	112.5
85	1424	.925	135
86	1472	.2	263
87	1473	.4	
88	1474	.5	
89	1475	.6	
90	1476	.7	
91			
92			
93			
94			
95			
96			
97			

TABLE 1. Continued
EXTERNAL TANK

CONSTANT SET 511

Ch. No.	T/C	X/L	θ	Ch. No.	T/C	X/L	θ	Ch. No.	T/C	X/L	θ
1	2089	.937	352.2	34	2120	.85	301.5	66	2152	.926	33.75
2	2088		289.4	35	2121	.86		67	2153		31.75
3	2087		250.6	36	2122	.87		68	2154		23.07
4	2090	.355	29.8	37	2123	.88		69	OPEN		
5	2091	.360		38	2124	.89		70	OPEN		
6	2092	.365		39	2125	.90		71	OPEN		
7	2093	.370		40	OPEN			72	2158	.926	355.2
8	2094	.355	23.08	41	2127	.925	301.5	73	OPEN		
9	2095	.36		42	2128	.935		74	2160	.926	345.2
10	2096	.365		43	2129	.82	292	75	2161		335
11	2097	.37		44	2130	.83		76	2162		330.2
12	2098	.355	20.98	45	2131	.84		77	2163		326.9
13	2099	.36		46	2132	.85		78	2164		324.5
14	2100	.365		47	2133	.86		79	OPEN		
15	2101	.37		48	2134	.87		80	2166	.441	31.43
16	2102	.355	17	49	2135	.88		81	2167	.425	337.5
17	OPEN			50	2136	.89		82	2168		345.6
18	2104	.40	330.2	51	2137	.91		83	2169		354
19	2105	.405		52	2138	.926		84	2170		5.63
20	2106	.41		53	2139	.930		85	2171		17
21	2107	.40	326.8	54	2140	.926	299.4	86	2172	.430	337.5
22	2108	.405		55	2141		270	87	2173		345.5
23	2109	.405	324.5	56	2142		258	88	2174		354
24	2110	.41		57	2143		250.6	89	2175		5.63
25	2111	.41	315	58	2144		247.5	90	2176		17
26	2112	.835	309.3	59	2145	.93	289.4	91	661	.415	11.25
27	2113	.820	305.4	60	2146		270	92	662	.42	
28	2114	.830		61	2147		258	93	663	.425	
29	2115	.835		62	2148		250.6	94	664	.43	
30	2116	.820	301.5	63	2149		247.5	95	665	.44	
31	2117	.830		64	2150	.935	270	96	666	.45	
32	2118	.835		65	2151		258	97	667	.455	
33	2119	.840									

TABLE 1. Concluded
EXTERNAL TANK

CONSTANT SET 522

Ch. No.	T/C	X/L	θ	Ch. No.	T/C	X/L	θ	Ch. No.	T/C	X/L	θ
1	668	.46	11.25	34	838	.80	270	66	945	.35	348
2	669	.47		35	839	.90	↓	67	946	.36	
3	670	.48		36	840	.23	292.5	68	947	.37	
4	671	.49		37	841	.25	↓	69	948	.375	
5	672	.50		38	842	.27	↓	70	949	.38	
6	673	.60		39	873	.07	315	71	950	.385	
7	674	.70		40	874	.08		72	951	.39	
8	675	.80	↓	41	875	.10		73	952	.395	
9	812	.40	258	42	876	.15		74	953	.40	
10	813	.23	270	43	877	.20		75	954	.405	
11	814	.24		44	878	.35		76	955	.41	
12	815	.25		45	879	.40		77	956	.415	
13	816	.27		46	880	.50		78	957	.42	
14	817	.29		47	881	.55		79	958	.425	
15	818	.30		48	882	.60		80	959	.43	
16	819	.31		49	883	.65		81	960	.44	
17	820	.32		50	884	.70		82	961	.445	↓
18	821	.325		51	885	.75		83	962	.45	
19	822	.33		52	886	.80	↓	84	2072	.42	36.32
20	823	.335		53	887	.84	↓	85	2073	.425	
21	824	.34		54	933	.926	337.5	86	2074	.43	
22	825	.345		55	934	.415	343.1	87	2075	.435	
23	826	.35		56	935	.42		88	2076	.45	
24	828	.36		57	936	.425		89	2077	.60	
25	829	.365		58	937	.43		90	2078	.65	
26	830	.37		59	938	.44		91	2079	.25	33.75
27	831	.375		60	939	.445		92	2080	.30	
28	832	.38		61	940	.45		93	2081	.375	
29	833	.39		62	941	.50		94	2082	.40	
30	834	.40		63	942	.60		95	2083	.43	
31	835	.50		64	943	.70		96	2084	.45	
32	836	.60		65	944	.80	↓	97	2085	.60	↓
33	837	.70	↓								

TABLE 2. TEST DATA SUMMARY

CONFIGURATION	MACH NUMBER	α_m' , deg	β , deg	CONSTANT SET								DATA GROUP NUMBERS				
				111	122	133	211	222	233	311	322	333	411			
OTS	3.01	0	0	25	230	28	3	220	5							
			3	29	231	32	9									
		-3	33	232	35	12										
		5					224									
		-5					225									
		5	0				226									
		5					227									
		-5					228									
		-5	0				221									
		5					222									
		-5					223									
	4.02	0	0	47	48	49	84	85	86							
		3	50	51	52	87										
		-3														
		4.5	53	54	55	90										
		-4.5	56	57	58	92										
		5					94									
		-5					95									
		7.5	59	60	61	97	98									
		-7.5	63	64	65	100	101	99								
		9														
		-9														

Table 2. Continued

CONFIGURATION	MACH NUMBER	α_m , deg	β , deg	DATA GROUP NUMBERS							
				CONSTANT SET							
OTS	4.02	5	0	111	122	133	211	222	233	311	322
		3	66	67	68	107	108	110	180	181	182
		-3				111			183	184	185
		4.5	69	70	71	112		135			213
		-4.5	72	73	74	136		137			
		5				138					
		-5				139					
		7.5	75	76	77	141	142	143	186	187	188
		-7.5	78	79	80	144	145	146	189	190	191
		9				147	148				
		-9				149					
		0				114					
		3	153	154	155	115	116	117	192	196	197
		-3				118			198	199	200
		4.5	156	157	158	119		120			
		-4.5	159	160	161	121		122			
		5				123					
		-5				124					
		7.5	162	163	164	126	127	128	201	202	203
		-7.5	165	166	167	129	130	131	205	206	207
		9				132	133				
		-9				134					

Table 2. Continued

CONFIGURATION	MACH NUMBER	α_m , deg	β , deg	DATA GROUP NUMBERS			
				111	122	133	511
OT	3.01	0	0	234	235	236	368
		3	262	263	264	387	369
		-3	265	266	267	389	388
		5	237	238	239	370	390
		-5	240	241	242	372	371
		5	0	243	244	245	374
		3	268	269	270	382	375
		3	399	400	401	391	392
		-3	402	403	404	393	394
		5	246	247	248	376	377
		-5	249	250	251	378	379
		-5	0	253	254	255	381
		3				395	396
		-3				397	398
		5	256	257	258	383	384
		-5	259	260	261	385	386

Table 2. Concluded

CONFIGURATION	MACH NUMBER	α_m , deg	β , deg	DATA GROUP NUMBERS					CONSTANT SET				
				111	122	133	511	522	323	324	364	365	366
OT	4.02	0	0	270	271	272	323	324					
			3										
			-3										
		5	273	274	275	325	326						
			5	276	277	278	327	328					
			0	279	280	281	329	330					
			3	282	283	284	331	332					
			-3	285	286	287	333	334					
		5	288	289	290	336	337						
			5	291	292	293	338	341					
			0	295	299	300	342	343					
			3	301	302	303	344	345					
			-3	314	315	316	346	347					
		5	317	318	319	348	349						
			5	320	321	322	350	353					
			-10	0	304	305	306	354	355				
			3				360	361					
			-3				362	363					
		5	307	308	309	356	357						
			-5	310	311	312	358	359					

Table 3. Equations for Calculating Local Surface Angle
of Attack on the Orbiter Model

Orbiter Thermocouple Numbers	Equation for Calculating δ
1 - 168 501 - 548	$\delta = \lambda + \alpha_m$
169 - 201 231 - 280	$\delta = \lambda - \alpha_m$
202 - 230 281 - 292 340 - 396	$\delta = \lambda + \text{Yaw}$
293 - 339	$\delta = \lambda$